

Au/Si(111): Analysis of the $(\sqrt{3} \times \sqrt{3})R 30^\circ$ and 6×6 structures by in-plane x-ray diffraction

D. Dornisch, W. Moritz, and H. Schulz

Institute of Crystallography and Mineralogy, University of Munich, Theresienstrasse 41, D-8000 München 2, Federal Republic of Germany

R. Feidenhans'l and M. Nielsen

Physics Department, Risø National Laboratory, DK-4000 Roskilde, Denmark

F. Grey

Max Planck Institute for Solid State Research, Heisenbergstrasse 1, D-7000 Stuttgart 80, Federal Republic of Germany

R. L. Johnson

II. Institute for Experimental Physics, University of Hamburg, Luruper Chaussee 149, D-2000 Hamburg 50, Federal Republic of Germany

(Received 18 December 1990)

In-plane, fractional-order diffraction-data sets from thin Au layers on Si(111) with $(\sqrt{3} \times \sqrt{3})R 30^\circ$ and 6×6 structures were measured at the wiggler beamline W1 at the Hamburg synchrotron radiation laboratory. For the $\sqrt{3} \times \sqrt{3}$ structure the trimer model is confirmed with an Au-Au distance of 2.8 Å. In the $\sqrt{3} \times \sqrt{3}$ unit cell, two additional sites beside the Au trimer were found which can be identified with distorted substrate layers or additional partially occupied Au sites. The 6×6 structure is a sixfold twinned structure. The observed Patterson function clearly indicates the main features of the structural units. Each consists of three trimer clusters of Au atoms, forming a nearly equilateral triangle. The local structure of each trimer is either the original $\sqrt{3} \times \sqrt{3}$ structure or a twin structure where the Au trimers are rotated by 60° . Three of these structural units form the 6×6 unit cell. Model calculations with incoherent superposition of twin domains lead to Patterson maps very similar to the one observed.

INTRODUCTION

Thin layers of Au on the clean Si(111) surface exhibit different reconstructions depending on the amount of Au deposited. In the literature there exist very different conclusions about the actual local coverage and the atomic arrangement in all the structures. The 5×1 structure has been reported to occur over the coverage range from 0.2 to 1.0 monolayer (ML). With increasing coverage it is gradually replaced by the $(\sqrt{3} \times \sqrt{3})R 30^\circ$ structure (in the following simply referred to as $\sqrt{3} \times \sqrt{3}$) starting at 0.7 ML. The $\sqrt{3} \times \sqrt{3}$ structure remains visible until 1.4 ML, accompanied by diffuse reflections in the pattern. Above 1.4 ML the diffraction pattern changes abruptly to a well-defined 6×6 pattern.¹ Other studies found coexistence of 5×1 and $\sqrt{3} \times \sqrt{3}$ structures between 0.5 and 0.8 ML, pure $\sqrt{3} \times \sqrt{3}$ between 0.8 and 0.95 ML, and 6×6 for 1 ML and above.²⁻⁴

For the $\sqrt{3} \times \sqrt{3}$ structure, two completely different types of models have been proposed which can be classified according to the coverage and symmetry of the adsorption site of the Au atoms. The first type has a coverage of $\frac{2}{3}$ ML and the Au atoms are located on $\frac{2}{3}$ of the threefold hollow sites (H_3) forming a honeycomb lattice with an empty H_3 site in the center of each hexagon. In this model there is no freedom of the lateral parameters. The nearest-neighbor distance within the surface plane is

given by the lattice parameter of the 1×1 unit cell of the substrate, i.e., 3.84 Å.³ In the second type of model a coverage of 1 ML is assumed and the Au atoms form trimer clusters at general sites. The center of the trimer defines the origin of the $\sqrt{3} \times \sqrt{3}$ superstructure cell. The distance between the Au atoms is about 2.0 Å, and corresponds to the nearest-neighbor distance in bulk Au.⁵ The registry of the Au atoms with respect to the substrate is not clear. Results from a recent medium-energy ion-scattering study⁶ favor the trimer model with the Au atoms not located on Si bulk sites. The results of this study are consistent with our results.

For the 6×6 structure, no definite model existed previously and only a few proposals concerning the local atomic arrangement have been published. Based on impact-collision ion-scattering spectroscopy (ICISS) measurements, Huang and Williams³ suggest a model which is consistent with the honeycomb model for the $\sqrt{3} \times \sqrt{3}$ structure. The 6×6 structure results from continuously putting more and more Au atoms onto the empty centers of the honeycombs of the ideal $\sqrt{3} \times \sqrt{3}$ structure and rearranging the unoccupied centers to form a 6×6 lattice. Coexistence of both structures would be possible. On a sample with a $\sqrt{3} \times \sqrt{3}$ LEED pattern, Salvan *et al.*⁷ observed by scanning tunneling microscopy (STM) surface areas exhibiting small units of the $\sqrt{3} \times \sqrt{3}$ structure which repeated with 6×6 periodicity. The 6×6

structure therefore seems to be a superstructure of the $\sqrt{3}\times\sqrt{3}$ structure and appears locally with increasing Au coverage.

From a LEED profile analysis of diffuse diffraction spots, Higashiyama, Kono, and Sagawa¹ drew the conclusion that with increasing Au coverage small areas of the $\sqrt{3}\times\sqrt{3}$ reconstruction are formed which are uncorrelated at an early state and finally are randomly distributed around the lattice points of a 6×6 lattice. Above 1.4 ML a well-defined 6×6 lattice is formed. They interpret the $\sqrt{3}\times\sqrt{3}$ structure as a disordered early stage of the 6×6 structure. Contrary to these studies in a more recent STM work, Nogami, Baski, and Quate⁴ found no coexistence between $\sqrt{3}\times\sqrt{3}$ and 6×6 phases. Additional Au atoms were soaked up by an expanding network of domain walls, proposed to be of the superheavy type, between antiphase domains of the $\sqrt{3}\times\sqrt{3}$ structure. In this way the domains become continuously smaller and beyond a critical coverage the surface rearranges to the 6×6 structure. When this happens, three of the small $\sqrt{3}\times\sqrt{3}$ domains form the unit cell of the 6×6 phase. The atomic arrangement within the structural unit is not resolved by the STM. In this work we present an in-plane structure analysis of the $\sqrt{3}\times\sqrt{3}$ superstructure by surface x-ray diffraction and a detailed atomic model of the 6×6 superstructure.

EXPERIMENT

The x-ray-diffraction experiments were performed on the vertical scattering diffractometer at the 32-pole wiggler W1 beamline at Hamburg Synchrotron Radiation Laboratory (HASYLAB).⁸ The Si(111) surfaces were prepared at the FLIPPER II photoemission beamline. The surfaces were cleaned by annealing to 900 °C and slowly cooling to produce a sharp 7×7 LEED pattern. The Au was evaporated onto the surface at a rate of 0.3 ML/min from an effusion cell held at 1180 °C. The surface was then transferred under UHV conditions to a small portable UHV x-ray cell, which was mounted on the diffractometer. The pressure in the cell was in the 10^{-10} -mbar region and no decay of intensities of the samples was observed over the measurement period (≈ 1 day). The samples were aligned on their optical surface by total reflection, such that the angle of incidence of the x rays to the surface could be kept fixed during data collection. In order to maximize the diffracted intensity and minimize the background the angle of incidence was set to the critical angle for total external reflection. The exit angle was near the critical angle, so the momentum transfer in the direction normal to the surface was close to zero, with the out-of-plane acceptance of the detector being 2°, corresponding to $q_z=0.28 \text{ \AA}^{-1}$. For the $\sqrt{3}\times\sqrt{3}$ structure 49 in-plane, integrated intensities for fractional-order reflections were collected. From these a set of 14 inequivalent structure-factor intensities was obtained. The reproducibility between symmetry-equivalent reflections was $\approx 10\%$, which was a measure of the systematic error. The uncertainty of the structure factor is the combination of the counting statistics and the systematic error. For the 6×6 structure data were collected for 139 inequivalent fractional-order reflections.

Reproducibility between symmetry-equivalent reflections was checked for six reflections giving again about 10% systematic error. The following analysis was performed using the fractional-order intensities. So the Patterson analysis only shows the correlation function of the differences to the 1×1 bulk structure.⁹ The positive peaks in the Patterson function can be interpreted as in-

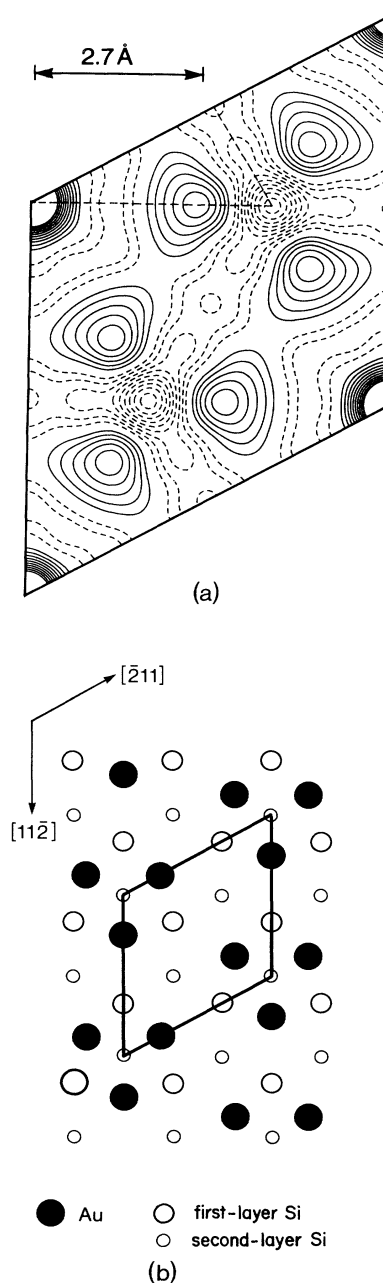


FIG. 1. (a) Patterson function of the $\sqrt{3}\times\sqrt{3}$ superstructure. The irreducible unit is marked by dashed lines. (b) Trimer model of $\sqrt{3}\times\sqrt{3}$ superstructure with undistorted first and second Si layers. One $\sqrt{3}\times\sqrt{3}$ unit cell is outlined. H_3 -like-adsorption sites for the Au atoms are assumed.

teratomic vectors in the superstructure. Structure refinement was performed with PROMETHEUS,¹⁰ which is capable of refining twinned structures. Because integer-order reflections are excluded from Fourier synthesis the registry between the superstructure and the underlying bulk lattice cannot be determined. The integer-order reflections were left off because of possible inhomogeneities of the surface. The small number of reflections would not allow definite conclusions about the registry.

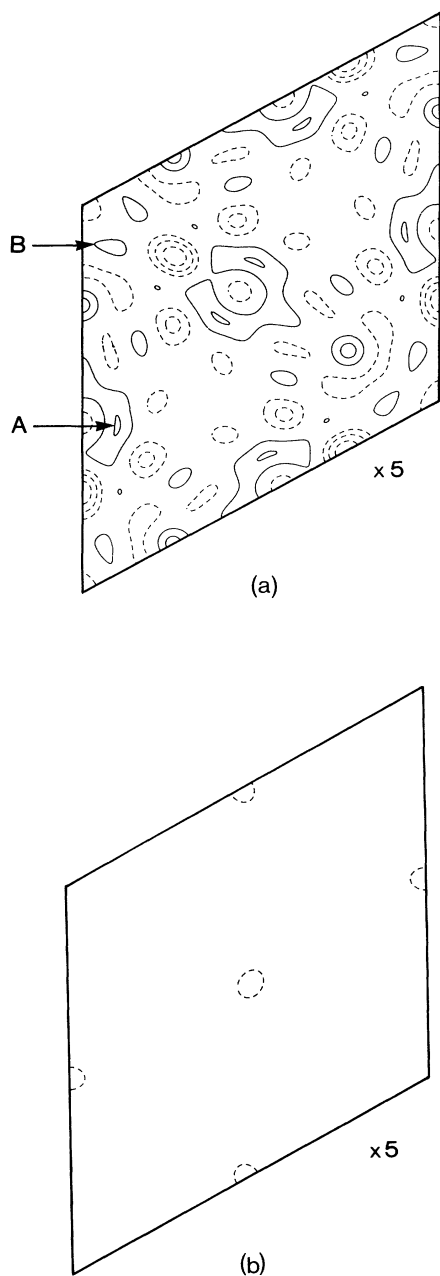


FIG. 2. (a) Residual-electron-density map of model I. (b) Residual-electron-density map of model III-Si and III-Au.

TABLE I. Relative weights of interatomic distance vectors in the system Au-Si.

Distance vector	$Z_1 \times Z_2$	Rel. weight
Au-Au	6241	1
Au-Si	1106	0.18
Si-Si	196	0.03

RESULTS

$(\sqrt{3}\times\sqrt{3})R30^\circ$ structure

Figure 1(a) shows the observed Patterson function. There is only one peak in the irreducible unit, corresponding to an interatomic vector of length 2.7 Å. From the relative weights of all possible distance vectors in the system Au/Si (Table I), it is evident that the observed vector represents a distance between Au atoms. Hence, the honeycomb models with Au atoms pinned at the threefold symmetry axis of the substrate lattice are incorrect. On the other hand, the parameters of all "heavy atoms" in the trimer model can be determined directly from the Patterson map. The Au atoms are located on the mirror planes of the $\sqrt{3}\times\sqrt{3}$ unit cell with symmetry $p31m$ [Fig. 1(b)]. Then the positions of the light atoms should come out by applying a difference Fourier synthesis to the heavy atom model. Refinement of this model gives a goodness of fit (GOF) (Ref. 11) of 189 and an R value of 0.21 (model I, Table II). The difference-electron-density map [Fig. 2(a)] shows two minor peaks *A* and *B* near two possible Si bulk lattice positions. When interpreting the residual electron density one has to keep in mind that Si gives only a minor contribution to the superstructure reflections and only becomes visible due to distortions from bulk lattice positions. Since the superstructure is noncentrosymmetric the true phases of the missing atoms may deviate significantly from those determined by the difference Fourier synthesis. Peak *A* may result from a shift of a substrate atom with a bulk lattice position at $(\frac{2}{3}, 0)$. [The coordinates are referenced to an origin at the center of the trimer as in Fig. 1(b)]. In the projected structure it looks as if the Si atom has moved into a bridge position between Au atoms of neighbored trimers. The distortion might occur in subsurface layers as well. To simplify further discussion we assume that the Au atoms are located near to H_3 sites, but our conclusions are independent of this assumption. The Si atom at $(\frac{2}{3}, 0)$ in the $\sqrt{3}\times\sqrt{3}$ superstructure cell is then the outermost of the top double layer. A shift to both sides of the mirror plane is required by symmetry and a split atom arises. The distance between the two split positions is about 0.96 Å. Full occupation with one Si atom improves the GOF to 114 and the R value to 0.11 (model II, Table II). As mentioned above, the adsorption site cannot be directly determined from the analysis without integer-order reflections, and the conclusions about the adsorption site are based on the assumption that peak *A* in Fig. 2(a) is originating from a silicon atom in the top-most substrate layer.

TABLE II. Comparison of different models of the $\sqrt{3}\times\sqrt{3}$ superstructure.

Model	Occupation of Site		Number of Parameters	GOF	σ -(GOF)	R
	A	B				
I			3	189	0.3	0.21
II	Si(0.68)		6	114	0.4	0.11
III-Si	Si(0.76)	Si(0.87)	8	0.9	0.4	0.055
III-Au	Si(0.81)	Au(0.16)	8	1.5	0.4	0.071

The interpretation of the second peak in the difference-electron-density map is not simple. It may result from a second distorted and incomplete substrate layer, or from a Au atom on top of the trimer or in a sub-surface position. In the second case the resulting, slightly distorted tetrahedra may be the first stage of formation of three-dimensional islands as expected after further growth of the epitaxial layer. The alternative interpretation of an incomplete substrate layer with atoms missing at $(\frac{1}{3}, \frac{2}{3})$ and $(\frac{2}{3}, \frac{1}{3})$, is supported by the work of Tanishiro and Takayanagi.¹² In a high-resolution electron microscopy study of the behavior of surface steps during epitaxial growth of Au on Si(111) they found that the density of Si substrate atoms in areas with 5×1 structure is only about 40% of that in unreconstructed areas. Similar observations were made for the $\sqrt{3}\times\sqrt{3}$ structure, but without quantitative measurements.

Putting an atom at the position of peak *B*, or on the mirror plane near peak *B* as well, removes this peak in the difference Fourier map. With Si at split position *A* and Si, or Au with a lower occupation factor corresponding to its larger number of electrons, in the mirror plane near peak *B*, the GOF drops to 0.9 ± 0.4 or 1.5 ± 0.4 and the *R* value to 0.055 or 0.071 for, respectively, the models III-Si or III-Au (Table II). All parameters were refined with exception of the isotropic Debye-Waller factor of the Si atoms which was fixed at its bulk value (Table III). The residual electron density is now very small [Fig. 2(b)] and the electron-density map of model III-Si is shown in Fig. 3. A list of the calculated and observed structure factors is given in Table IV.

The occupation factors of the different sites and possible conclusions about the Au coverage need to be discussed. In the structure-refinement calculation only relative occupation factors can be determined. Keeping the

Au coverage fixed at 1 ML and putting Si on the two split positions *A* and *B* [Fig. 2(a)] results in these positions being overoccupied. The small distance between the split positions does not allow more than $\frac{1}{2}$ Si atom at site *A* and $\frac{1}{3}$ Si at site *B*. Attempts to fix these values in the refinement process led to poor convergence and to a considerably larger GOF. Therefore, the deviation from the ideal coverages must be considered as significant, although a precise determination of occupation factors is, in general, problematic because of the strong coupling between temperature factors and occupation factors. The overoccupation of the Si sites could have two explanations. It is possible that more than one Si layer is distorted, or the Au layer might not be complete. The second possibility agrees qualitatively with a recent medium-energy ion-scattering (MEIS) experiment⁶ where a Au coverage of 0.84 was found for the $\sqrt{3}\times\sqrt{3}$ structure. If Si is placed at site *B* within the Au trimer with an occupation factor of $\frac{1}{3}$ then site *A* can only be occupied by 38% Au which is too low. It appears more plausible to partially fill site *B* with Au. In this case site *A* is occupied with at most 50% Si, and our data yield $\theta_{\text{Au1}}=0.62$ and $\theta_{\text{Au2}}=0.010$. The total Au coverage is still lower than the value of $\theta_{\text{Au}}=0.84$ determined by MEIS,⁶ but it is within the error limits and within the stability range of the $\sqrt{3}\times\sqrt{3}$ structure. The empty trimer sites may be statistically distributed or located in domain boundaries, but this cannot be ascertained and determined from the x-ray-diffraction analysis. In STM pictures there is no indication of statistically missing trimers in ordered domains so domain boundaries or steps are the most probable locations. In general, the picture of missing trimers in domain boundaries is consistent with the fact that $\sqrt{3}\times\sqrt{3}$ diffraction spots are always slightly diffuse, as described in detail in Ref. 1.

TABLE III. Parameters of the best $\sqrt{3}\times\sqrt{3}$ models. (Refined parameters are underlined.)

Model	Atom	<i>x</i>	<i>y</i>	θ	<i>B</i>
III-Si	Au(1)	<u>0.243</u> ₁	0.000	1.0	<u>4.0</u> ₂
	Si(2)	<u>0.125</u> ₅	0.000	<u>0.87</u> ₈	0.5
	Si(1)	<u>0.643</u> ₅	<u>0.082</u> ₅	<u>0.76</u> ₉	0.5
III-Au	Au(1)	<u>0.243</u> ₂	0.000	1.0	<u>4.0</u> ₃
	Au(2)	<u>0.129</u> ₁₀	0.000	<u>0.16</u> ₃	4.0
	Si(1)	<u>0.645</u> ₆	<u>0.085</u> ₆	<u>0.81</u> ₁₃	0.5

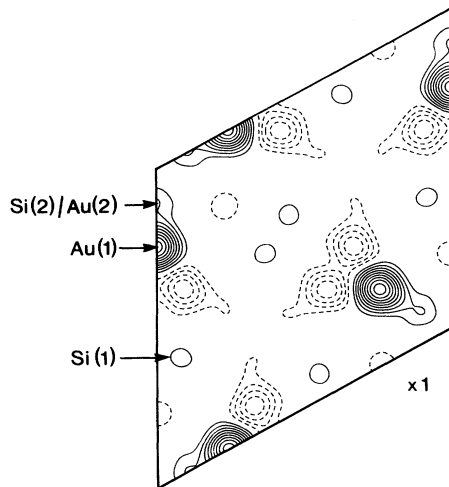


FIG. 3. Electron-density map of model III-Si. (The electron-density map of model III-Au looks exactly similar.)

as described in detail in Ref. 1.

The distortions in the outermost substrate layer are responsible for the reduction of the GOF from 189 down to about 1, the value expected for a correct model within the experimental error limits. The triangular shape of the peaks observed in the Patterson function is also a consequence of these distortions. The distorted substrate layer Si1 may be interpreted as a result of the tendency of Si atoms to go into bridge positions between Au atoms. The splitting is then caused by the two equivalent positions due to the symmetry of the substrate leading to two domains.

6×6 structure

Figure 4 shows the observed 6×6 Patterson function. As in the $\sqrt{3}\times\sqrt{3}$ structure, the peaks are due to Au-Au interatomic vectors. In fact, it can be seen that the complete set of Patterson vectors of the $\sqrt{3}\times\sqrt{3}$ structure appears in the 6×6 Patterson map (shaded area in Fig. 4). This means that the local atomic arrangement is very similar and clustering of Au into trimers is the basic

TABLE IV. Observed and calculated intensities of the $\sqrt{3}\times\sqrt{3}$ structure (F_{obs}^2 is scaled to the sum of F_{calc}^2).

(a) Model III-Si					
H	K	F_{obs}^2	F_{calc}^2	$(F_{\text{obs}}^2 - F_{\text{calc}}^2) / \sigma(F_{\text{obs}}^2)$	
0	1	8903	8708	0.3679	
1	2	19 865	20 724	-0.7025	
2	3	2958	2957	0.0061	
3	4	140	79	0.9699	
0	2	1397	1365	0.4816	
1	3	624	656	-0.6215	
2	4	1117	943	0.5793	
3	5	226	201	0.6402	
0	4	5549	6760	-1.0047	
1	5	2110	2210	-0.3067	
2	6	47	48	-0.0077	
0	5	831	834	-0.0543	
1	6	1318	1073	1.0563	
0	7	61	45	0.4204	
(b) Model III-Au					
H	K	F_{obs}^2	F_{calc}^2	$(F_{\text{obs}}^2 - F_{\text{calc}}^2) / \sigma(F_{\text{obs}}^2)$	
0	1	9037	8828	0.3892	
1	2	20 165	21 264	-0.8857	
2	3	3003	3120	-0.4679	
3	4	142	143	-0.0171	
0	2	1418	1373	0.6655	
1	3	634	667	-0.6414	
2	4	1133	809	1.0670	
3	5	230	193	0.9192	
0	4	5633	6642	-0.8249	
1	5	2142	1963	0.5365	
2	6	48	62	-0.3209	
0	5	844	851	-0.1707	
1	6	1338	1047	1.2383	
0	7	61	1	1.5760	

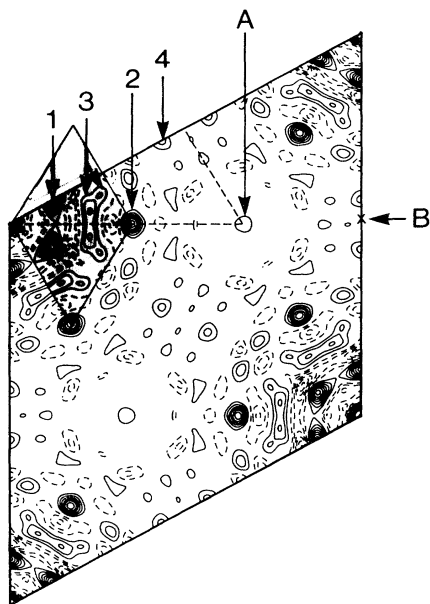


FIG. 4. Patterson function of the 6×6 superstructure. The shaded area corresponds to a $\sqrt{3} \times \sqrt{3}$ unit cell. The interpretation of peaks 1–3 is given in Table V. At position *B* no peak is observed and the peak at position *A* is negligibly small.

structural element in both structures. Therefore, most peaks of the 6×6 Patterson function can be identified at this stage (Table V). Peak 1 represents the Au-Au distance within one trimer. As in the $\sqrt{3} \times \sqrt{3}$ structure, the peak has a triangular shape due to contributions from distorted substrate layers. Peak 2 can be attributed to a lattice vector of the $\sqrt{3} \times \sqrt{3}$ structure, i.e., the trimer-trimer distance, and finally peak 3, which represents vectors between nonequivalent Au atoms of neighbored trimers, is slightly split and smeared out. The position of the maximum in the Patterson function does not give exactly the interatomic distance because of (1) superposition of slightly different interatomic distance vectors and (2) evaluation of only the superstructure reflections in this

analysis. So only differences to the 1×1 structures are observed. Consequently negative peaks occur where distance vectors exist in the bulk structure, but not in the superstructure and the maxima can be slightly shifted by superposition with such negative peaks. Most important is the fact that some peaks are missing in the Patterson map of the 6×6 structure. No indication is found of distance vectors with twice the trimer-trimer distance of the original $\sqrt{3} \times \sqrt{3}$ structure at $(\frac{1}{3}, \frac{2}{3})$ (*A*), or three times this distance at $(1, \frac{1}{2})$ (*B*) nor to a distance along the longer diagonal of the $\sqrt{3} \times \sqrt{3}$ unit cell at $(\frac{1}{2}, \frac{1}{2})$ (see Fig. 4). This distance vector is symmetry equivalent to vector *B* due to the inversion symmetry of the Patterson function. Taking into account all features of the Patterson map, the structural unit of the 6×6 superstructure seems to be an incomplete $\sqrt{3} \times \sqrt{3}$ cell where one of the trimers, namely, that on $(0,1)$ of the original $\sqrt{3} \times \sqrt{3}$ lattice, is missing. The $\sqrt{3}$ periodicity must be distorted exactly after one single $\sqrt{3} \times \sqrt{3}$ period. Putting this structural unit onto the origin of a 6×6 lattice produces a unit cell with symmetry $p3$ [model *T1*, Fig. 5(a)]. The mirror plane of the substrate symmetry $p3m1$ is destroyed and two twin domains arise. The diffracted intensities from both domains can be superposed coherently or incoherently. Refinement of this structure model assuming incoherent superposition exhibits poor convergence and terminates with an extraordinary high *R* value of 0.67, but leads to a calculated Patterson function which is in fact similar to the one observed [Fig. 5(b)]. In comparison, the same calculation with coherent superposition inevitably leads to a calculated Patterson function with additional peaks, caused by the interatomic vectors between trimers of different twin domains [Fig. 5(c)].

The suggestion of incoherent superposition of the twin domains in the 6×6 structure is supported by the argument that a system which forces the atoms to arrange in a large superstructure cell, like the 6×6 structure, can be assumed to form spatially extended domains as well. The theoretical coverage of the first model is $\theta_{\text{Au}} = 0.25 \text{ ML}$, which is obviously too low, so more Au atoms have to be put into the 6×6 unit cell. Nogami, Baski, and Quate⁴ present a STM photograph of the 6×6 reconstructed surface showing a corresponding periodic arrangement of

TABLE V. Interpretation of the Patterson peaks of 6×6 structure (see Fig. 4).

Peak No.	<i>d</i>	Equivalent distance vector in $\sqrt{3} \times \sqrt{3}$ structure
1	2.8 Å	Au-Au distance within one trimer.
2	6.8 Å	Distance between equivalent Au atoms in one $\sqrt{3} \times \sqrt{3}$ unit cell and those in the next-neighbor cell of the original $\sqrt{3} \times \sqrt{3}$ structure.
3		Distance between nonequivalent Au atoms of different trimers.
4		Not identified.
<i>A</i>	$2a\sqrt{3}$	Distance between equivalent Au atoms in one $\sqrt{3} \times \sqrt{3}$ unit cell and those in the second next-neighbor cell.
<i>B</i>	$3a\sqrt{3}$	Distance between equivalent Au atoms in one $\sqrt{3} \times \sqrt{3}$ unit cell and those in the third next-neighbor cell.

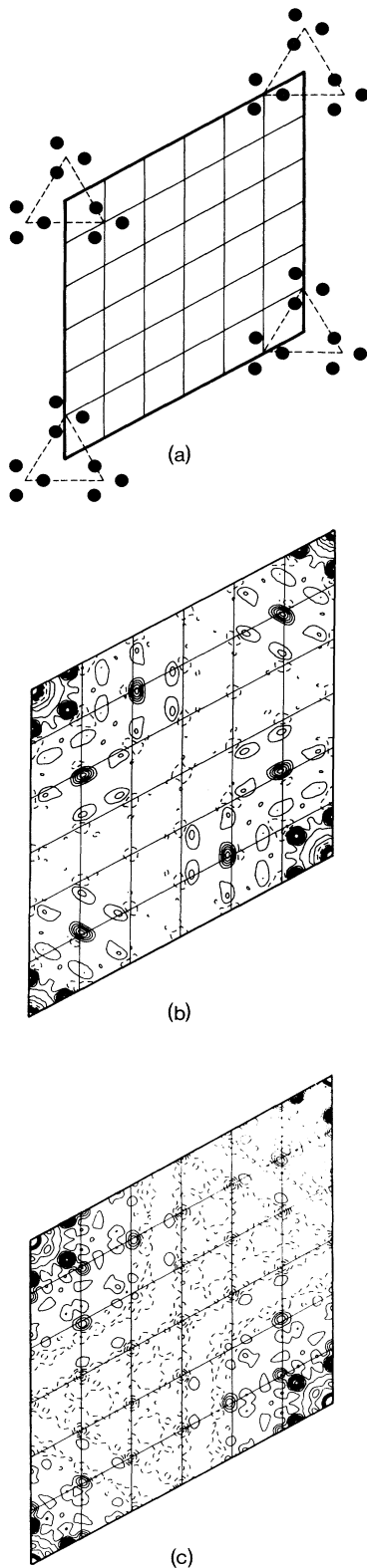


FIG. 5. (a) Single twin domain of model $T1$. (b) Calculated Patterson function with incoherent superposition of twin domains. (c) Calculated Patterson function with coherent superposition of twin domains.

three groups of Au atoms at the edges of the 6×6 unit cells, and moreover two additional similar triple groups, rotated by 60° , inside the 6×6 unit cell. The detailed atomic structure within the groups could not be resolved by the STM. From the analysis of the $\sqrt{3}\times\sqrt{3}$ structure we identify the structures to be Au trimers.

To reproduce the observed Patterson function with such an arrangement the $\sqrt{3}\times\sqrt{3}$ periodicity between the three triple groups has to be destroyed. This condition can only be fulfilled if each of the triple groups belongs to a different antiphase domain of the former $\sqrt{3}\times\sqrt{3}$ structure. From bond-length considerations only two trimer triplets can belong to different $\sqrt{3}\times\sqrt{3}$ antiphase domains in a single 6×6 unit cell, depicted as $A1$ and $A2$ in Figs. 6 and 7(a). If the third orientation of the trimer-triplet $A3$ were present in the 6×6 unit cell at the same time, then domain walls of the superheavy type would occur. The trimers on both sides of the wall would then overlap with one common Au atom. However, no interatomic vector characteristic of this W-shaped cluster appears in the observed Patterson function. Therefore, the third triple group must belong to a different type of $\sqrt{3}\times\sqrt{3}$ domain. There exists an alternate arrangement of Au atoms if the trimer is shifted to another threefold axis inside the 1×1 unit cell with a rotation of 60° . One domain of this type is shown in Fig. 6 ($B1$). It corresponds to a domain of the $\sqrt{3}\times\sqrt{3}$ structure having changed registry from H_3 -like sites for the Au atoms to T_4 -like sites. We assume that both arrangements of Au atoms occur in the 6×6 structure. Some remarks should be made about the local density of Au atoms in the domain walls. In order to preserve the Au trimers as structural units of the $\sqrt{3}\times\sqrt{3}$ superstructure the domain walls between antiphase domains (type $A-A$) must always have a lower local Au-atom density than the perfect $\sqrt{3}\times\sqrt{3}$ structure, otherwise the Au-Au distance becomes too small. On the other hand, at walls between

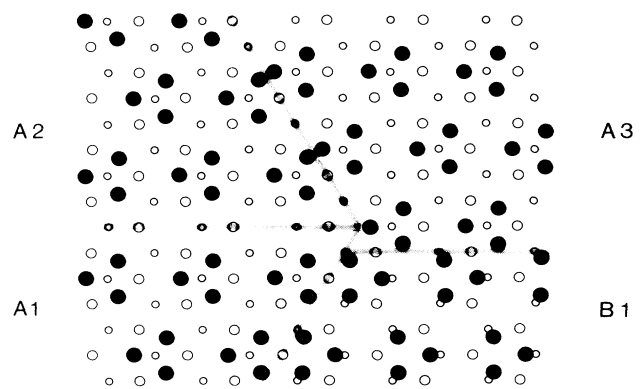


FIG. 6. Atomic arrangement of possible " $\sqrt{3}\times\sqrt{3}$ domains." Light walls between domains $A1$ and $A2$, superheavy walls between $A2$ and $A3$, heavy walls between $A1$ and $B1$ or $A3$ and $B1$.

“twin” domains (type *A-B*) the local Au-atom density is increased. A combination of trimer triplets in the described manner causes a modulation of the Au-atom density within the 6×6 unit cell. It is worth noting that a stacking fault in the substrate, as is the case for the Si(111) 7×7 reconstruction, would be a reason for a 60° rotation of the trimers preserving registry with respect to deeper layers. But there would be no shift of the trimer

centers and just this seems to be an important feature of the structure. Structure refinements starting with models without this shift fail to converge.

Within one 6×6 unit cell the different types of trimer triplets can appear in six different combinations, which maintain the distortion of the $\sqrt{3}\times\sqrt{3}$ periodicity between the Au trimers. In Table VI all possible combinations of three trimer triplets within a 6×6 unit cell are

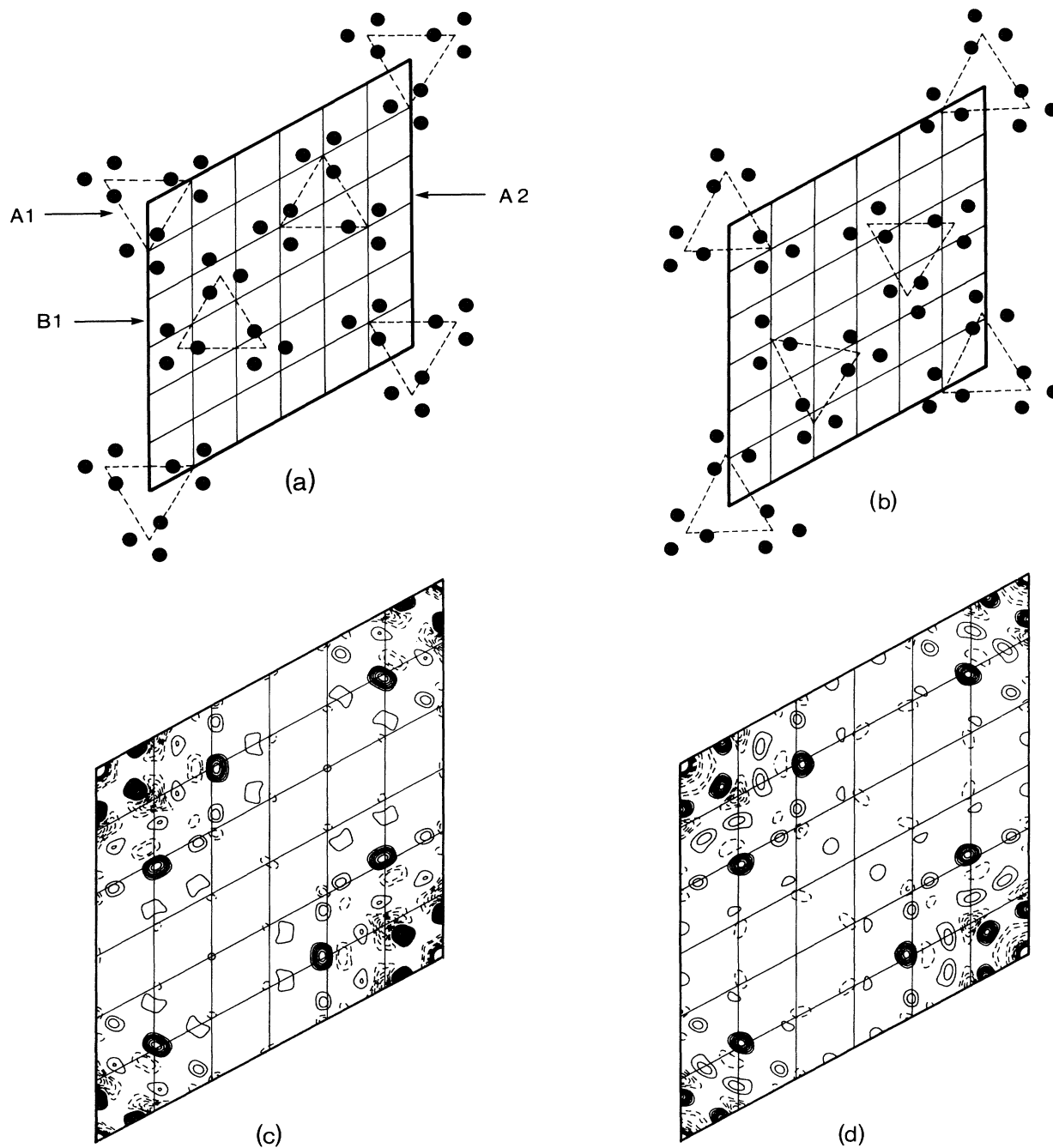


FIG. 7. (a) Single twin domain of model *T3* with starting positions of the trimers. (b) Refined positions of model *T3-2*. (c) Calculated Patterson function of model *T3-1*. (d) Calculated Patterson function of model *T3-2*.

TABLE VI. Possible combinations of structural units (s.u.) (i.e., trimer triplets) from different " $\sqrt{3} \times \sqrt{3}$ domain types" within one single 6×6 unit cell.

Type of domain of s.u. at position			Excluded by Patterson function	Excluded by bond length	Allowed
(0,0)	$(\frac{1}{3}, \frac{2}{3})$	$(\frac{2}{3}, \frac{1}{3})$			
A1	A2	A3	—		
A1	A2	B1			+
A1	A2	B2			+
A1	A2	B3			+
A1	B1	A2			+
A1	B1	B1	—		
A1	B1	B2		—	
A1	B1	B3		—	
A1	B2	A2			+
A1	B2	B1		—	
A1	B2	B2	—		
A1	B2	B3		—	
A1	B3	A2			+
A1	B3	B1		—	
A1	B3	B2		—	
A1	B3	B3	—		

listed. Those which lead to a Patterson function that does not agree with the one observed and those with Au-Au distances that are obviously too small have been excluded from the structural refinement. The remaining combinations represent the six twin domains of the 6×6 superstructure, which are reduced to symmetry $p1$. The twin operations are the threefold axis, and the mirror plane of the initial $p3m1$ symmetry of the substrate. One 6×6 unit cell with its structural units of type $A1$, $A2$ and $B1$ is shown in Fig. 7(a).

In the first step of the structure refinement only rigid trimers were considered which were allowed to shift laterally and to change their size. One isotropic overall Debye-Waller factor and incoherent superposition was assumed (model $T3-1$). This resulted in a calculated Patterson function which agrees well with the one observed [Fig. 7(c)], but the R value remained at a very high value of 0.475. It drops to 0.380 when all atomic coordinates are allowed to move freely (model $T3-2$). The resulting distortions of the trimers are not considered to be significant due to the high standard deviations [Fig. 7(b), Table VII] and the fact that the calculated Patterson function did not change significantly [Fig. 7(d)]. A very large contribution to the R value comes from four intensities at very small momentum transfer. Eliminating these intensities reduces the R value to 0.271, but produces no significant change in the refined parameters. The reason for the deviation may be a systematic error in the measurement, or additional structural parameters which could not be taken into account in this model because of the limited number of measured intensities. The large 6×6 unit cell combined with the low $p1$ symmetry restricts the number of parameters of the model to the coordinates of one single Au layer. In the analysis of the $\sqrt{3} \times \sqrt{3}$ structure the initial model with one Au layer (model I, Table II) gave a similarly high R value of 0.21 which decreases to 0.055 on introducing two additional

partially occupied sites. In the $\sqrt{3} \times \sqrt{3}$ analysis it was found that the triangular shape of the Patterson peak results from the overlap of the main Au(1)-Au(1) vector with weaker vectors due to Au(1)-Si(1) and Au(1)-Au(2)/Si(2). The similar shape of the corresponding Au-

TABLE VII. Parameters of the best 6×6 model ($T3-2$).

Atom	x	y	θ	B
Au(1)	0.268	0.037	1.0	1.8 ₆
Au(2)	0.159 ₃₀	0.054 ₃₀	1.0	1.8
Au(3)	0.144 ₃₁	-0.077 ₂₄	1.0	1.8
Au(4)	0.071 ₂₇	0.200 ₃₁	1.0	1.8
Au(5)	-0.041 ₂₅	0.219 ₂₄	1.0	1.8
Au(6)	-0.058 ₂₃	0.093 ₂₄	1.0	1.8
Au(7)	0.912 ₂₉	0.868 ₂₉	1.0	1.8
Au(8)	0.793 ₂₉	0.871 ₃₁	1.0	1.8
Au(9)	0.786 ₂₉	0.746 ₂₇	1.0	1.8
Au(10)	0.370 ₂₄	0.523 ₂₄	1.0	1.8
Au(11)	0.256 ₂₉	0.536 ₃₀	1.0	1.8
Au(12)	0.245 ₂₈	0.409 ₂₈	1.0	1.8
Au(13)	0.220 ₂₅	0.720 ₂₄	1.0	1.8
Au(14)	0.099 ₃₀	0.712 ₂₆	1.0	1.8
Au(15)	0.095 ₂₉	0.587 ₂₂	1.0	1.8
Au(16)	0.592 ₂₅	0.867 ₂₅	1.0	1.8
Au(17)	0.448 ₂₃	0.863 ₃₀	1.0	1.8
Au(18)	0.463 ₂₆	0.750 ₂₆	1.0	1.8
Au(19)	0.605 ₃₀	0.073 ₃₂	1.0	1.8
Au(20)	0.619 ₂₇	0.196 ₂₇	1.0	1.8
Au(21)	0.488 ₂₄	0.082 ₂₅	1.0	1.8
Au(22)	0.424 ₂₇	0.248 ₂₉	1.0	1.8
Au(23)	0.456 ₂₄	0.377 ₂₄	1.0	1.8
Au(24)	0.322 ₂₅	0.264 ₂₆	1.0	1.8
Au(25)	0.776 ₂₃	0.423 ₂₆	1.0	1.8
Au(26)	0.743 ₂₃	0.531 ₂₅	1.0	1.8
Au(27)	0.662 ₂₄	0.396 ₂₄	1.0	1.8

Au peak in the 6×6 Patterson function (peak 1 in Fig. 4) indicates that additional layers are reconstructed in the 6×6 structure. It should be noted that the observed Patterson function can only be reproduced if the characteristic features of the structure are present as discussed above. This fact, together with the observation of a similar arrangement of structural units by the STM topograph of Nogami, Baski, and Quate,⁴ is a strong argument for the proposed model.

The coverage in the model shown in Fig. 7 is 0.75 ML, which disagrees with the observation that the 6×6 structure occurs at coverages above 1 ML. Hence additional atoms have to be included between the trimers or perhaps in deeper layers of the substrate. However no indication of these atoms was found in the Patterson function. The introduction of additional sites would increase the number of variable parameters beyond the limit for which a reliable determination is possible.

CONCLUSION

We conclude that the main features of the 6×6 structure are Au trimer triplets arranged in the way shown in Fig. 7(b), with additional Au sites in between. The refined 6×6 structural model fits well into the general picture of Au on Si(111) that has emerged from our work and other recent studies.

1. The trimer model for the $\sqrt{3} \times \sqrt{3}$ superstructure is confirmed. The Au-Au distance determined from the Patterson function is not found in any of the other models discussed in the literature. Refining the $\sqrt{3} \times \sqrt{3}$ tri-

mer model leads to $\text{GOF} = 1.5 \pm 0.4$ or 0.9 ± 0.4 and $R = 0.071$ or 0.055 for the two structure models III-Si or III-Au. The Au-Au distance found is 2.80 ± 0.02 Å, which is slightly less than the bulk bond length of Au.

2. The Au coverage cannot be determined absolutely from the x-ray superstructure reflections alone, however our results are in good agreement with a medium energy ion scattering study⁶ and this technique is known to yield accurate coverage measurements. The coverage of the $\sqrt{3} \times \sqrt{3}$ structure is less than 1 ML due probably to missing trimers in domain boundaries.

3. The 6×6 superstructure is a sixfold twinned structure, with $p1$ symmetry of the twin domains. The 6×6 phase is not an ordered superstructure of the $\sqrt{3} \times \sqrt{3}$ structure, but results from considerable rearrangement of some of the Au atoms and probably also substrate atoms. The reasons for this rearrangement may be either a modulation of the local Au density which allows better compensation of the strain induced by the adsorbate layer, or a stacking fault in the substrate similar to the Si(111) 7×7 reconstruction.

ACKNOWLEDGMENTS

We thank Professor D. Wolf and Dr. H. Meyerheim for useful discussions, Dr. J. Schneider and R. Rossmann for support in the adaption of PROMETHEUS to surface structure problems, and the staff of HASYLAB for their help. Part of this work was supported by the BMFT (Grant Nos. 0546IAB8 and 05490CAB) and the Danish National Research Council.

¹K. Higashiyama, S. Kono, and T. Sagawa, *Jpn. J. Appl. Phys.* **25**, L117 (1986).

²G. Le Lay, *Surf. Sci.* **132**, 169 (1983).

³J. H. Huang and R. S. Williams, *Phys. Rev. B* **38**, 4022 (1988).

⁴J. Nogami, A. A. Baski, and C. F. Quate, *Phys. Rev. Lett.* **65**, 1611 (1990).

⁵K. Oura, M. Katayama, F. Shoji, and T. Hanawa, *Phys. Rev. Lett.* **55**, 1486 (1985).

⁶M. Chester and T. Gustafsson, *Phys. Rev. B* **42**, 9233 (1990).

⁷F. Salvan, H. Fuchs, A. Baratoff, and G. Binnig, *Surf. Sci.* **162**, 634 (1985).

⁸R. Feidenhans'l, F. Grey, M. Nielsen, and R. L. Johnson, in

Kinetics of Ordering and Growth at Surfaces, edited by M. G. Lagally (Plenum New York, 1990), p. 189.

⁹M. J. Buerger, *Vector Space and its Applications in Crystal-structure Investigation* (Wiley, New York, 1959).

¹⁰U. H. Zucker, E. Perenthaler, W. F. Kuhs, R. Bachmann, and, H. Schulz, *J. Appl. Crystallogr.* **16**, 358 (1983).

¹¹ $\text{GOF} = \chi^2 / (N - p)$; with $\chi^2 = \sum [(F_{\text{obs}}^2 - F_{\text{calc}}^2) / \sigma^2(F_{\text{obs}}^2)]$ and $\sigma(\text{GOF}) = 1 / \sqrt{(N - p)}$; N : number of observables, p : number of parameters. $R = (\{\sum [w(F_{\text{obs}}^2 - F_{\text{calc}}^2)^2] / \sum (wF_{\text{obs}}^4)\})^{1/2}$; $w = 1 / \sigma^2(F_{\text{obs}}^2)$.

¹²Y. Tanishiro and K. Takayanagi, *Ultramicroscopy* **31**, 20 (1989).